MODULATION TRANSFER FUNCTION OF STEREO PARTICLE IMAGE VELOCIMETRY TECHNIQUE

R. Giordano, T. Astarita, G. M. Carlomagno
DIAS - University of Naples "Federico II" - p.le Tecchio 80, 80125 Naples – Italy

Keywords: *Stereo Particle Image Velocimetry, PIV data processing*

Abstract

A theoretical analysis of the spatial resolution in terms of Modulation Transfer Function (MTF) of the Stereo Particle Image Velocimetry (PIV) technique with and without the correction of the misalignment error is performed and results show that some wavelengths of the flow field can be significantly dephased and modulated. A performance assessment has been conducted with synthetic images and shows a good agreement with the theoretical analysis. The reconstruction of the three-dimensional displacement field is achieved using both the methods proposed by Soloff et al. [1] and by Willert [2].

1 Introduction

The Stereo PIV technique allows obtaining three components planar velocity measurements by using two bi-dimensional PIV flow fields. Nowadays, there are different methods to implement this technique; Prasad [3] subdivided these methods into geometric and calibration-based approaches. The latter is the most accurate one and it is possible to categorise it in further approaches: the first is based on the procedure introduced by Soloff et al. [1] and the second is that proposed by Willert [2]. In the former approach a mathematical relation which computes the three-component (3C) reconstruction in a single step is proposed. On the other hand, in the Willert's approach, the reconstruction of the three-dimensional displacement field is done by means of geometrical considerations, i.e. local viewing angles of each camera in every point of the measurement plane (i.e. laser sheet).

In all calibration-based approaches an accurate calibration, which permits to correct the error in perspective and the possible distortion caused by the lenses, is essential to obtain good results in the measurement of the velocity components. Typically, calibration is obtained setting a calibration pattern, which contains a grid of marks regularly spaced along two orthogonal directions, in one or more positions along the z direction (orthogonal to the plane); ideally, the position $z = 0$ (hereafter named calibration plane) is the position of the light sheet, i.e. the measurement plane. In the calibration procedure, a mapping function is computed, which allows to transform the object coordinates (x, y, z) into the image coordinates (X_1,Y_1) and (X_2,Y_2) of the two cameras; coefficients of the mapping function are normally calculated with the least squares method.

A drawback of the Stereo PIV technique is the impossibility to set the laser sheet exactly in the $z = 0$ position. An adjusting procedure based on a cross-correlation between the images of the two cameras, recorded in the same instant, has been proposed by many authors. Results present in the literature have shown that the correction of misalignment errors isn't needed for a uniform displacement field; for this reason non-uniform ones are herein simulated. They consist of a single one dimensional sinusoidal shear displacement, with various wavelengths. The Stereo PIV technique applied to the latter displacement type shows that a decrease of the wavelength produces a decrease of the measured sine wave amplitude. For this purpose, the spatial resolution in terms of Modulation Transfer Function is investigated by varying the

wavelength of the sinusoidal component and by using synthetic images.

2 Stereo Particle Image Velocimetry technique

As already mentioned, in this study the measurements are obtained using the reconstruction of the 3C displacement field based on both the methods proposed by Soloff et al. [1] and Willert [2]. The common procedure consists of the following steps:

- Calibration is achieved to correct errors in perspective and distortions caused by lenses: a mapping function which transforms the object coordinates (x, y, z) into the image coordinates (X_1, Y_1) of camera 1 and (X_2, Y_2) of camera 2 is computed.
- The misalignment between calibration and measurement planes is evaluated.
- The 3C displacement field is computed.

2.1 Calibration

Nowadays, different calibration models are used: camera pinhole models and interpolating function-based ones. The camera pinhole model, proposed by Tsai [4], is made up of 6 extrinsic and 6 intrinsic parameters. The former describes the position of the camera pinhole in object space by means of a translation vector and a rotation matrix. Intrinsic parameters are specific to the camera: pixel aspect ratio; radial distortion factors (first and second order) which describe the distortion caused by the lenses; focal length; intersection of the optical axis with the image plane. For the second type of calibration model, a generic interpolating function can be chosen.

In the work presented here, only the polynomial function of third order in x and y and second order in z has been used. The procedures used to obtain Stereo PIV measurements can be applied with any other mapping functions, as long as the calibration is 3D, i.e. camera pinhole model or any 3D interpolating function. The reason of this condition is in the necessity to have a volume mapping which contains the measurement plane.

2.2 Correction procedure of misalignment

As already mentioned, when real Stereo PIV measurements are made, one of the major problems is the unavoidable misalignment which occurs between the calibration plane and the laser sheet, i.e. the measurement plane. Generally, an offset along the z direction and a rotation around the x and y axis form this misalignment.

By neglecting this misalignment, one commits the following errors:

- Position error: 3C displacement reconstruction is made using two-components (2C) vectors relative to two different positions.
- 3C-reconstruction error: in the 3C reconstruction proposed by Soloff et al. [1], the local gradient matrix is computed in a wrong point, and this, in turn, causes a wrong displacement vector (see Sect. 2.3); in the 3C reconstruction proposed by Willert [2], the local viewing angles are calculated in an erroneous position, so they cause a mistake in the evaluation of 3C displacement vectors (see Sect. 2.3).

The correction procedure adopted here is explained in details in Giordano and Astarita [5].

2.3 Reconstruction of the three components

With the approach proposed by Soloff [1] first the 2C displacement fields are evaluated for the two cameras with a standard PIV algorithm applied to the warped images; then, the 3C displacement field is computed with a procedure that includes in one step the images de-warping and the 3C reconstruction. This procedure consists in the evaluation of the mapping function gradient, for both cameras. The resulting system is linear with three unknowns and four equations.

As regard the Willert's reconstruction [2], the warping approach has been used (see

Coudert and Schon [6]), i.e. the images are first de-warped, by using the mapping function obtained in the calibration step, then a standard PIV algorithm is applied to both images on a common grid to compute the two–component displacement field for each camera. A further precaution has been adopted, in order to reduce the loss of image quality and, then, of the 3C displacement field: images de-warping is made inside the iterative deformation PIV process, according to Scarano et al. [7] and Wieneke [8].

Once the two 2C displacement fields relative to the two cameras are obtained, the 3C reconstruction is done by means of geometrical consideration. The formulas proposed by Willert [2] are:

$$u = \frac{u_1 tan\alpha_2 - u_2 tan\alpha_1}{tan\alpha_2 - tan\alpha_1} \quad (1)$$

$$w = \frac{u_1 - u_2}{tan\alpha_2 - tan\alpha_1} \quad (2)$$

$$v = \frac{v_1 tan\beta_2 - v_2 tan\beta_1}{tan\beta_2 - tan\beta_1} = \frac{v_1 + v_2}{2} + \frac{w}{2}\left(tan\beta_1 + tan\beta_2\right) \quad (3)$$

where the viewing angles were evaluated by measuring the relative distances between the measurement point and the cameras (see Fig. 1 for the viewing angles description).

Here the viewing angles have been computed by means of the formulas proposed by Giordano and Astarita [5]:

$$tan(\alpha_c) = \frac{Y_z^{(c)} X_y^{(c)} - Y_y^{(c)} X_z^{(c)}}{Y_y^{(c)} X_x^{(c)} - Y_x^{(c)} X_y^{(c)}} \quad (4)$$

$$tan(\beta_c) = \frac{Y_z^{(c)} X_x^{(c)} - Y_x^{(c)} X_z^{(c)}}{Y_x^{(c)} X_y^{(c)} - Y_y^{(c)} X_x^{(c)}} \quad (5)$$

where $X^{(c)}$ is the mapping function for the image coordinate X_c relative to camera c and the subscript indicates derivation.

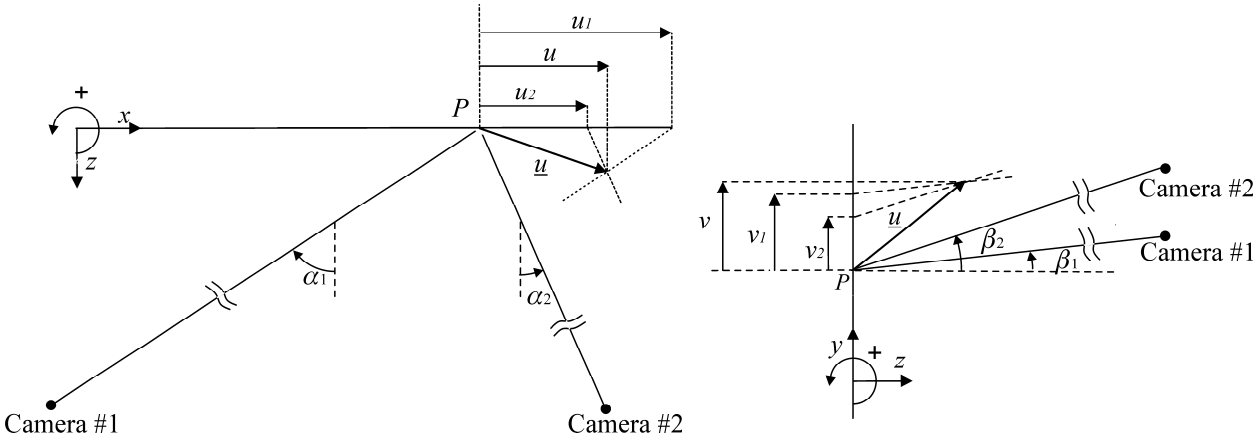

Fig. 1. Geometric reconstruction used by Willert [2]

3 Synthetic images

Measurements are carried out using synthetic images. They are generated including the effect of perspective and distortion caused by the viewing angle of the cameras, set in an angular stereoscopic configuration.

The geometrical and optical configurations are simulated by using the camera pinhole model proposed by Tsai [4]. Obviously, both calibration and PIV images are generated with the same configuration parameters.

The light sheet has a Gaussian shape and also the distribution of the particles' dimension is Gaussian, whereas the distribution of the particles is uniform in the whole light sheet. On average, the particles have a size of 2-3 *pixels* in the image. Their shape is supposed to be Gaussian and, then, the intensity level is computed by integrating the particle light distribution on each image pixel; really if two or

more particles overlap, the intensity level of each pixel is the sum of the intensity of each particle. The pixels have a maximum level of 4095 and a unit fill factor. The dimension of the images is 1280x1024 *pixels*.

The viewing angles of the two cameras are -45° and +45°, whereas the mean distance between each camera and the measurement plane is equal to 520*mm*. The mean resolution along the *y* direction is 14.6*pixels/mm* and along the *x* direction is about 10.2*pixels/mm*.

In this analysis, the PIV images have been investigated by using the iterative image deformation method (IDM) described by Astarita [9], where the standard cross correlation and the top hat moving average approach (THMA) have been used.

4 Theoretical analysis of the modulation transfer function

The aim of this section is to analyse the Modulation Transfer Function of the Stereo PIV technique through investigation of the effects caused by two different parameters: the laser thickness and the linear dimension of the interrogation window *W* (i.e. the modulation associated to the PIV process).

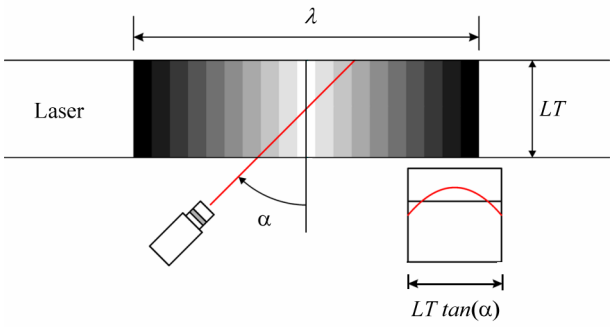

Fig. 2. Sketch of the modulation associated to the laser thickness.

As far as the laser thickness is concerned, the modulation happens in the image recording. Let's consider a sinusoidal component along *x* direction with wavelength λ and laser thickness *LT*. By neglecting the gradients in *y* and *z* directions, in the image recording the sinusoidal signal is filtered by means of a top hat moving window filter with width equal to $LT \cdot tan(\alpha)$, where α is the local viewing angle (see Fig. 2). Then frequency response is the sinc function:

$$MTF_{LT} = sinc\left(\frac{LT \cdot tan\,\alpha}{\lambda}\right) \qquad (6)$$

In order to study the influence of *W* on the MTF of the technique, let's consider a displacement field consisting of a single sinusoidal component with several wavelengths and a very small laser thickness, that allows to neglect the above mentioned effect. On account of the method chosen to evaluate the PIV images (IDM with THMA approach, see Sec. 3), the theoretical MTF of the PIV technique used herein should be practically equal to the one of the top hat moving window filter; the latter, for the typical values of the interrogation window dimensions and of the wavelengths used in PIV measurements, is practically coincident with $\mathrm{sinc}(W/\lambda)$, where *W* is the linear dimension of the square interrogation window.

The analysis showed by Giordano and Astarita [5] led to neglecting, for common configurations, the modulation relative to the 3C reconstruction for both approaches.

In order to extend the theoretical analysis of the MTF relative to the Stereo PIV technique with a misalignment between the calibration and measurement planes, let's consider a misalignment consisting of a translation along *z* equal to 1*mm*. For a displacement field consisting of a sinusoidal component along the y direction, the misalignment above described doesn't bring any appreciable error. This happens because the position error implies the use of two 2C-vector in the 3C reconstruction translated along *x* and practically coincident, since the sinusoidal component recurs along the *x* direction. On the other hand, the 3C reconstruction error is negligible for the misalignment contemplated here.

For the aforesaid reason, it is chosen to simulate a displacement field that consists of a *v* component sinusoidal along the *x* direction, for which the position error is relevant, since in this case the sinusoidal component recurs along the *y* direction. The amplitude of the sinusoidal component is equal to 0.10*mm* and the wavelength varies between 1.6*mm* and 12*mm*. The linear dimension of the square interrogation

window is 16*pixels* and the overlap has been chosen equal to 2*pixels* in order to avoid further modulation.

For this displacement field the position error implies the combination of two dephased sinusoidal components in the 3C reconstruction and so a further modulation. For this purpose, let's consider the reconstruction formulas for the *v*-component (Eq. 3) used in 3C reconstruction proposed by Willert [2]; for the displacement field simulated, it becomes (w = 0):

$$v = \frac{v_1 + v_2}{2} \tag{7}$$

So, if in a generic point a misalignment Δz occurs between calibration and measurement planes, two dephased sinusoidal component are used in the reconstruction, instead of the correct component $sin(kx)$, where $k=2\pi/\lambda$:

$$v = \frac{sin[k(x+t_1)] + sin[k(x+t_2)]}{2} \tag{8}$$

The two phases t_1 and t_2 are:

$$t_c = -\Delta z \cdot tan(\alpha_c) \quad c = 1,2 \tag{9}$$

where Δz is the local misalignment and α_c is the viewing angle of camera c (see Fig. 3).

By manipulating Eq. 8, it is possible to find:

$$\begin{aligned} v &= \frac{1}{2}[cos(kt_1) + cos(kt_2)]sin(kx) \\ &+ \frac{1}{2}[sin(kt_1) + sin(kt_2)]cos(kx) \\ &= MTF_{\Delta z}\, sin[kx + \varphi] \end{aligned} \tag{10}$$

where:

$$MTF_{\Delta z} = \begin{cases} abs\{\cos[k(t_1 - t_2)/2]\} \\ for \quad \cos(kt_1) + \cos(kt_2) \geq 0 \\ -abs\{\cos[k(t_1 - t_2)/2]\} \\ for \quad \cos(kt_1) + \cos(kt_2) < 0 \end{cases} \tag{11}$$

$$\varphi = arctan\{tan[k(t_1 + t_2)/2]\} \quad , \tag{12}$$

$$\varphi \in \left]-\frac{\pi}{2}, \frac{\pi}{2}\right[$$

So, instead of the correct component $sin(kx)$, one measures a modulated and dephased sinusoidal component, with modulation factor $MTF_{\Delta z}$ and phase φ.

In Fig. 4 the $MTF_{\Delta z}$ as a function of W/λ is shown, for the stereoscopic set-up used: it's interesting to note that $MTF_{\Delta z}$ can be even negative for particular values of W/λ.

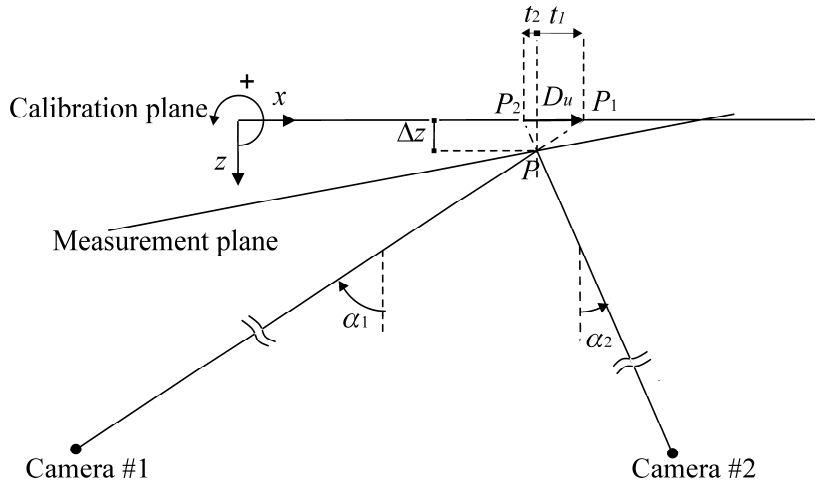

Fig. 3. Sketch of a generic misalignment error between calibration and measurement planes.

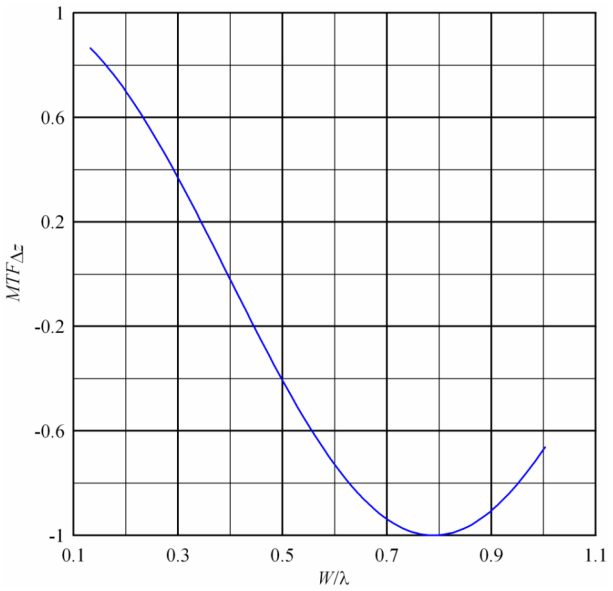

Fig. 4. $MTF_{\Delta z}$ as a function of W/λ for the stereoscopic set-up used with a misalignment $\Delta z=1mm$.

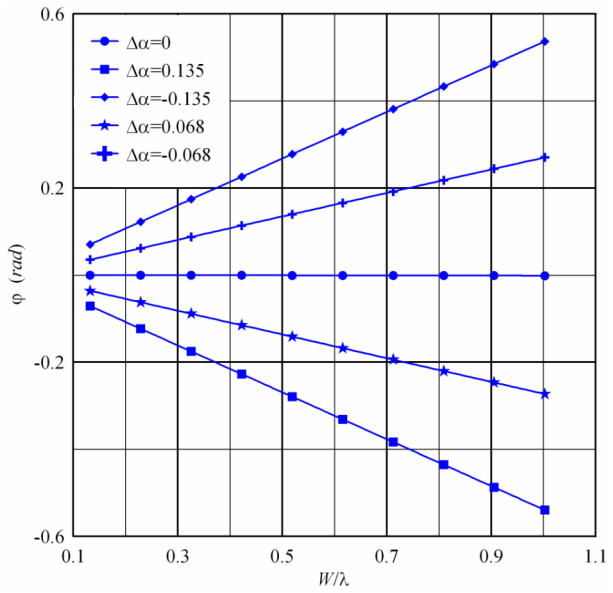

Fig. 5. φ as a function of W/λ for various $\Delta\alpha = |\alpha_2| - |\alpha_1|$ (*rad*) and the stereoscopic set-up used with a misalignment $\Delta z=1mm$

The $MTF_{\Delta z}$ function for the used configuration doesn't vary in an appreciable manner for the small variation of the difference between the absolute values of the viewing angles $\Delta\alpha = |\alpha_2| - |\alpha_1|$; for this reason only one curve is shown. On the other hand, the phase value is very sensible to the latter difference. For this reason, in Fig. 5 φ as a function of W/λ is shown for different values of $\Delta\alpha$. Since the configuration adopted here is symmetric, the maximum value of the latter difference is identical (in absolute value) at the right and left extremities of the image plane.

5 Performance assessment

In this section the performance assessment of the theoretical analysis of the Modulation Transfer Function will be shown. Both effects caused by the laser thickness and the linear dimension of the interrogation window W will be considered. For the latter one, only the effect due to misalignment between calibration and measurement planes will be shown, since the irrelevance of the modulation associated to the stereoscopic reconstruction on the spatial resolution is widely discussed in Giordano and Astarita [5].

5.1 MTF due to laser thickness

In order to validate the Eq. 6, a displacement field with the v component sinusoidal along x direction with amplitude $0.1mm$ and wavelength equal to $12mm$ has been simulated, whereas the laser thickness ranges from $0mm$ to $18mm$. Obviously, this range includes thickness too large physically speaking; this choice is done only to verify the Eq. 6. The stereoscopic set-up is the same described in Sec. 3.

Fig. 6 shows the theoretical curve (solid line) and the ones obtained with both Soloff and Willert approaches (circle and triangle symbols, respectively): these are nearly coincident with theoretical one and substantially coincident each other.

Fig. 7 shows total and random errors for both approaches: the total error is the quadratic mean of the error committed in the evaluation of the sinusoidal component in each point of the measurement plane; whereas, the random error indicates only the error made with respect to the modulated sinusoidal component. The difference between them is the error associated with the modulation. The overlapping of the curves relative to the two approaches for both total and random errors is a further proof that this kind of modulation is associated to the image recording and, then, it doesn't' depend on the 3C reconstruction approach.

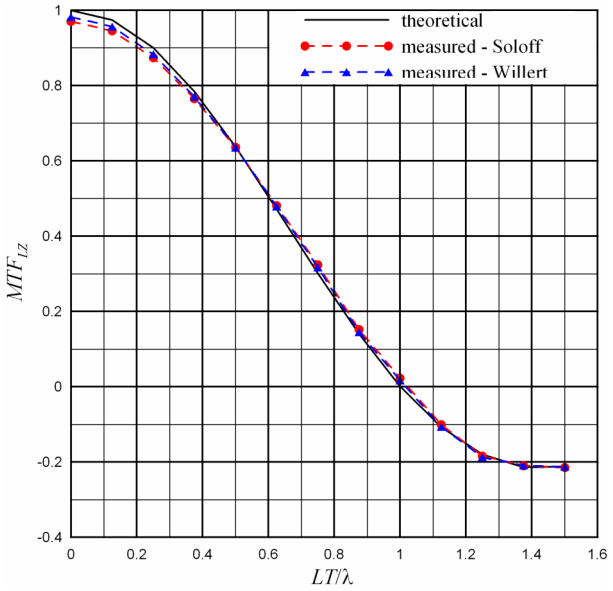

Fig. 6. MTF_{LZ} as a function of LT/λ for the stereoscopic set-up used with a wavelength $\lambda = 12mm$.

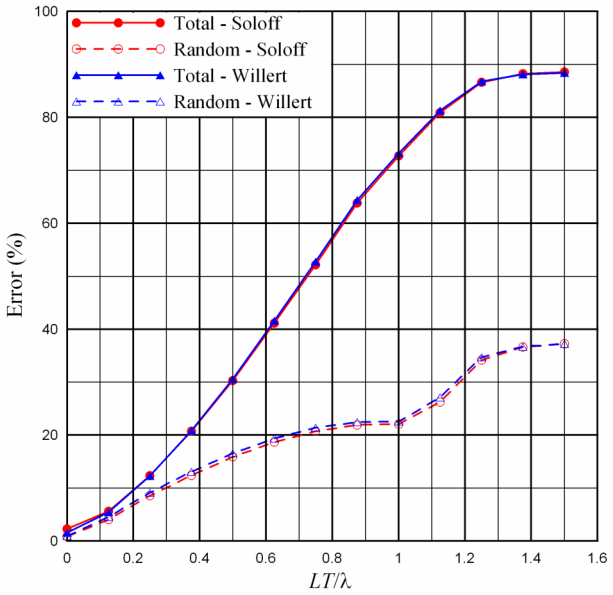

Fig. 7. Total and random errors as a function of LT/λ for the stereoscopic set-up used with a wavelength $\lambda = 12mm$.

5.2 MTF due to interrogation window

Fig. 8 shows the MTF for both approaches applied with and without correction of the misalignment errors, in addition to the theoretical curves (solid lines for both approaches applied with and without correction).

For the Soloff's approach (red curves), it can be seen a substantial coincidence of the theoretical curve (solid) with the curves related to the procedure applied with correction (closed circle), whereas the Willert's curve is slightly below the theoretical one (closed triangle). The curves relative to the procedure applied without correction of misalignment are both in good agreement with the theoretical ones (open circle and open triangle for the procedures proposed by Soloff et al. [1] and Willert [2] respectively).

In Figs. 9 and 10 the total and random errors committed in both approaches are shown. The error curves associated to both configurations show a smaller random error for the Willert's approach with respect to the Soloff's one, both applied with and without correction of the misalignment errors, whereas the total errors are quite similar. The curves relative to the procedures applied without correction show normally, as espected, higher errors with respect to the one obtained with correction.

It has to be evidenced that the errors associated to the misalignment of the measuring plane is not a consequence of the normal Stereo PIV modulation, but would be even higher if an higher resolution method was used in PIV process.

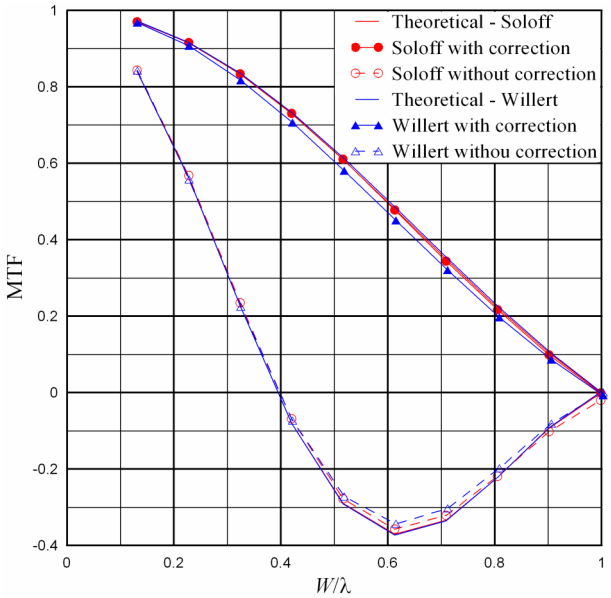

Fig. 8. *MTF* as a function of W/λ. Curves without symbols refer to theoretical values. Circles and triangle are relative to procedures proposed by Soloff et al. [1] and Willert [2] whereas closed and open symbols refer to values measured with and without correction of misalignment error, respectively.

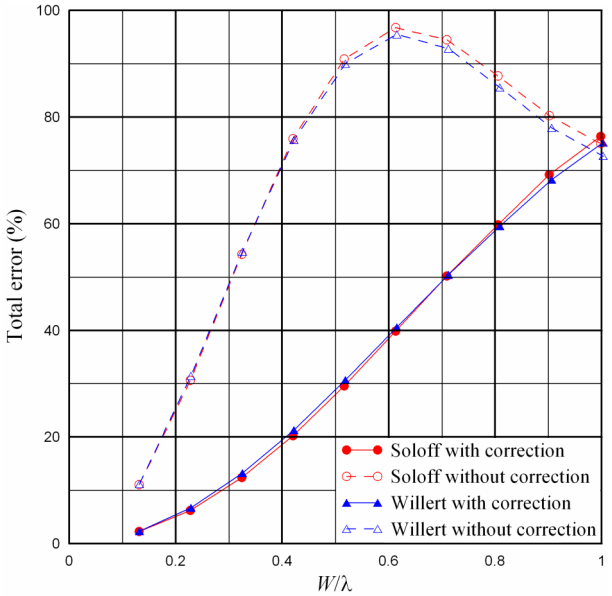

Fig. 9. Total errors as a function of W/λ. Circles and triangle are relative to procedures proposed by Soloff et al. [1] and Willert [2] whereas closed and open symbols refer to values measured with and without correction of misalignment error, respectively.

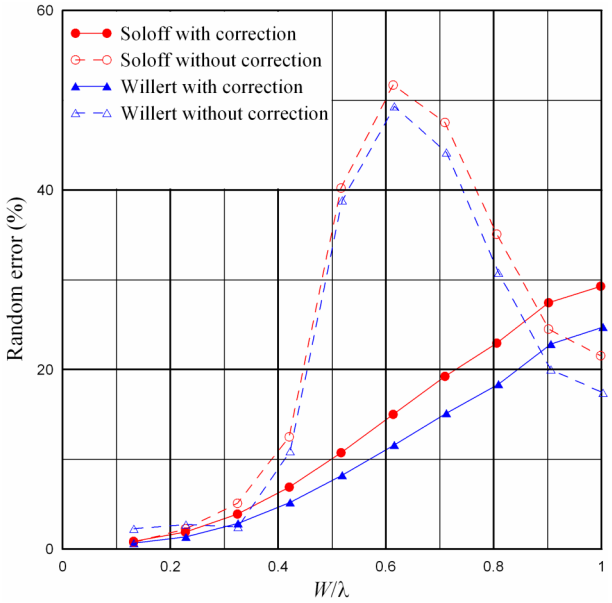

Fig. 10. Random errors as a function of W/λ. Circles and triangle are relative to procedures proposed by Soloff et al. [1] and Willert [2] whereas closed and open symbols refer to values measured with and without correction of misalignment error, respectively.

6 Conclusions

The Stereo PIV technique applied with both the procedures proposed by Soloff et al. [1] and Willert [2] has been investigated by simulating non-uniform displacement fields. These consisted of a sinusoidal component with various wavelengths. This choice permitted to analyse the spatial resolution of the technique. Since the measured sine amplitude decreases with the reduction of the wavelength, the results have been showed in terms of Modulation Transfer Function (MTF) as a function of the normalised spatial wavelength.

The investigation of the spatial resolution associated to the laser thickness showed the range of spatial wavelengths measurable with good accuracy. The performance assessment has been conducted with synthetic images and confirmed this analysis.

The theoretical analysis of the MTF associated with the misalignment error between the calibration and measurement planes led to concluding that, depending on the stereoscopic set-up used, some wavelengths of the flow field can be dephased and modulated, even with a negative modulation modulus. The performance assessment conducted with both Soloff and Willert approaches showed a good agreement with the theoretical MTF.

References

[1] Soloff S, Adrian R and Liu Z. Distortion compensation for generalized stereoscopic particle image velocimetry. *Meas Sci Technol*, Vol. 8, No. 12, pp 1441-1454, 1997.

[2] Willert C. Stereoscopic digital particle image velocimetry for application in wind tunnel flows. *Meas Sci Technol*, Vol. 8, No. 12, pp 1465-1479, 1997.

[3] Prasad A. Stereoscopic particle image velocimetry. *Exp Fluids*, Vol. 29, No. 2, pp 103-116, 2000.

[4] Tsai RY. A Versatile Camera Calibration Technique for High-Accuracy 3D Machine Vision Metrology Using Off-the-Shelf TV Cameras and Lenses. *IEEE Journal of Robotics and Automation 4*, Vol. RA-3, No. 4, pp 323-344, 1987.

[5] Giordano R and Astarita T. Stereo PIV applied to non-uniform simulated displacement fields. *Proc 7th International Symposium Particle Image Velocimetry*, Rome (Italy), CD file directory: piv2007\Papers\Stereo PIV 1\Giordano.pdf., 2007.

[6] Coudert SJM and Schon JP. Back-projection algorithm with misalignment corrections for 2D3C stereoscopic PIV. *Meas Sci Technol*, Vol. 12, No. 9, pp 1371-1381, 2001.

[7] Scarano F, David L, Bsibsi M and Calluaud D. S-PIV comparative assessment: image dewarping + misalignment correction and pinhole + geometric

projection. *Exp Fluids*, Vol. 39, No. 2, pp 257-266, 2005.

[8] Wieneke B. S Stereo-PIV using self-calibration on particle images. *Exp Fluids*, Vol. 39, No. 2, pp 267-280, 2005.

[9] Astarita T. Analysis of interpolation schemes for image deformation methods in PIV: effect of noise on the accuracy and spatial resolution. *Exp Fluids*, Vol. 40, No. 6, pp 977-987, 2006.

Copyright Statement